High-pressure Raman and x-ray diffraction studies on LaB_6

B. K. Godwal,[1] E. A. Petruska,[2] S. Speziale,[3] J. Yan,[4] S. M. Clark,[1,4] M. B. Kruger,[2] and R. Jeanloz[1,5]
[1]*Department of Earth & Planetary Sciences, University of California, Berkeley, California 94720, USA*
[2]*Department of Physics, University of Missouri, Kansas City, Missouri 64110, USA*
[3]*Deutsches GeoForschungsZentrum (GFZ), Telegrafenberg, 14473 Potsdam, Germany*
[4]*Advanced Light Source, Lawrence Berkeley National Laboratory, 1 Cyclotron Road, Berkeley, California 94720, USA*
[5]*Department of Astronomy, University of California, Berkeley, California 94720, USA*
(Received 9 March 2009; revised manuscript received 22 October 2009; published 19 November 2009)

X-ray diffraction measurements and Raman spectroscopy at room temperature document the equation of state and the frequency shifts for E_g, T_{2g}, and A_{1g} vibrational modes of polycrystalline LaB_6 under pressure. The data exhibit smooth pressure dependencies, yielding a zero-pressure isothermal bulk modulus $K_{0T}=164(\pm 2)$ GPa in good accord with independent ultrasonic measurements, and show no evidence of structural or electronic phase transitions up to at least 25 GPa.

DOI: 10.1103/PhysRevB.80.172104 PACS number(s): 61.50.Ks, 64.30.−t, 71.20.−b, 71.10.Hf

The rare-earth hexaborides RB_6, which have been the subject of intense theoretical and experimental study,[1–4] crystallize in the CaB_6 type structure with the rare-earth (R) atom and the octahedral B_6 molecules populating a CsCl-type structure.[5] Band-structure calculations show that there is a finite energy gap between the conduction and valence bands that can contain 20 electrons per unit cell.[6,7] As six B atoms provide 18 electrons, the rare-earth metal hexaboride should be electrically insulating if the metal is divalent and metallic if R is trivalent.

The band structure of LaB_6 is characterized by wide boron *sp* bands and La *sd* bands.[8,9] The La *d* bands are near the Fermi level (E_F), and there is strong hybridization of the La *d* and B *sp* bands.[8,9] In LaB_6, in particular, considerable charge transfer is expected from La to B atoms because La is a trivalent metal. Hence, despite its ionic character, LaB_6 should exhibit (semi) metallic behavior and this is confirmed by electrical resistivity measurements.[9,10]

The lattice dynamics of LaB_6 have been studied experimentally by neutron inelastic scattering,[11] and the small observed value of the elastic constant c_{12} is explained by incorporating a volume-dependent force acting on the La atoms.[12] These long-range forces arise from the occupied part of the conduction band formed by the antibonding orbitals of the B_6 molecule and the $5d$ e_g orbitals of the La atoms.[12] Trends in the c_{12} and c_{44} values of mixed-valence $Sm_{1-x}Y_xS$ (Ref. 13) with variable metal size, as well as divalent YbB_6, show that the volume dependence of the long-range forces can lead to violations of the Cauchy relation and a small value of c_{12}.[11,12]

Previous high-pressure Raman and angle-dispersive x-ray diffraction (ADXRD) measurements showed evidence of LaB_6 undergoing a phase transition around 10 GPa.[14] The present study is aimed at investigating the nature of the high-pressure phase transition, and determining the structure of the phase. First-principles electronic structure calculations reveal an electronic topological transition near this pressure.[14] High-pressure experiments are needed because of the subtle nature of such transitions, and their appearance as band crossovers with varying temperature or impurities. We used LaB_6 in powdered form for both Raman and x-ray measurements, in contrast with the earlier work in which the Raman measurements were carried out on single crystals while ADXRD was from powder. All of our experiments were performed at room temperature, and we improved the precision over past high-pressure x-ray diffraction experiments by carrying out high-resolution measurements at the Advanced Light Source of the Lawrence Berkeley National Laboratory. These studies are also of interest because the monovalent nonmagnetic LaB_6 is of great technological importance.[15]

Powder samples of LaB_6 with particle size ~ 10 μm were loaded in a Mao-Bell type diamond-anvil cell with a 4:1 mixture of methanol:ethanol to reduce nonhydrostatic stresses, and a small amount ($<5\%$) of ruby powder for pressure measurements. Diamond anvils with 350 μm culets were used for compression and spring-steel gaskets with sample chamber diameters of ~ 150 μm contained the sample, ruby, and methanol:ethanol mixture between the diamonds. Raman spectra were collected in a backscattering geometry. The 514.5 nm line of an argon-ion laser was used for excitation, with 27 mW incident on the diamond anvil. A Kaiser supernotch plus filter was used to separate the laser line from the Raman-scattered light, which was dispersed with a Spectrapro 500i spectrograph, and detected with a Spec-10 liquid-nitrogen-cooled CCD detector. Raman spectra were collected with a resolution of 2 cm^{-1} up to a pressure of 20 GPa.

LaB_6 powder was compressed between two diamond anvils with 230 μm culets, using a 16:3:1 (volume ratio) mixture of methanol-ethanol-water (MEW) as the pressure-transmitting medium; some experiments were also performed with no pressure medium. A 10 μm size fragment of Au foil and a few specks of ruby were loaded into a ~ 120 μm diameter sample chamber drilled out of a 250-μm-thick stainless steel foil that had been indented to a final thickness of ~ 45 μm.

High-pressure experiments were performed using a short symmetric piston-cylinder diamond-anvil cell (DAC) at beamline 12.2.2 of the Advanced Light Source.[16] Powder x-ray diffraction patterns were collected in angle-dispersive geometry using monochromatic radiation ($\lambda = 0.485\,94 \pm 0.000\,04$ Å) and a MAR345 image-plate detector at a distances of either 295.540 (± 0.001) or

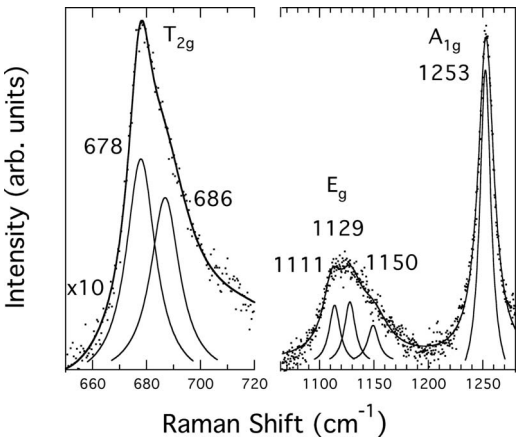

FIG. 1. Raman spectrum of LaB_6 at ambient pressure, showing T_{2g} (678 cm^{-1}), E_g (1118 cm^{-1}), and A_{1g} (1253 cm^{-1}) modes. Solid lines correspond to Lorentzian fits to the experimental data.

380.116($\pm$0.001) mm from the sample. The x-ray beam size was approximately 100 μm in maximum dimension. Pressure was determined by the ruby-fluorescence method and by x-ray diffraction of Au,[17–19] and the sample-to-detector distance was calibrated by collecting the diffraction pattern of powdered LaB_6 at ambient conditions. The software package *FIT2D* (Ref. 20) was used both for beam-position and sample-to-detector distance calibrations, and for collapsing the two-dimensional diffraction images into one-dimensional patterns. Ten well-resolved (nonoverlapping) peaks of LaB_6 were observed in the diffraction patterns collected from experiments performed with the MEW pressure medium.

As the previous high-pressure Raman and x-ray diffraction studies on LaB_6 used ethanol-methanol as a pressure-transmitting medium, and had indicated a subtle phase transition around 10 GPa, we examined the possible effects of nonhydrostaticity due to freezing of the pressure medium by collecting data from a sample with argon as pressure medium (125 μm diameter sample chamber in a Re gasket indented to a final thickness of 70 μm, and mounted in a symmetric cell having 300 μm size culets).[21] In these experiments, the x-ray beam size was approximately 10 μm across and we could clearly observe the (100), (110), (111), (200), (210), (211), (220), (300), (310), and (311) diffraction lines to a pressure of 16 GPa.

The three main Raman peaks expected for LaB_6 at ambient pressure are observed at 678 cm^{-1} (T_{2g}), 1129 cm^{-1} (E_g), and 1253 cm^{-1} (A_{1g}) (Fig. 1 and Table I). In agreement with most previous work,[5,22,23] we do not observe a mode at 438 cm^{-1} as reported in the single-crystal Raman study of Ref. 14. The A_{1g} and E_g vibrations are B-B bond-stretching modes and T_2 is an angle-bending mode of the boron lattice. The high-frequency shoulder of the T_{2g} mode is likely due to the presence of both B^{11} and B^{10} isotopes (underlying peaks at 678 and 686 cm^{-1}), and the E_g mode is best fit with a triplet at frequencies of 1111, 1219, and 1150 cm^{-1}. In the previous single-crystal study, the E_g mode was fit with a doublet and only one T_{2g} mode (around 678 cm^{-1}) was tracked with pressure.[14]

The T_{2g} peaks at 678 and 686 cm^{-1} at ambient pressure, shift linearly with pressure up to 20 GPa at rates of 3.6($\pm$0.1) and 3.7($\pm$0.1) cm^{-1}/GPa, respectively (Table I and Fig. 2). As expected, their pressure dependencies are indistinguishable. Close examination of the frequency shift of the 686 cm^{-1} peak suggests nonlinearities at $\sim$4 and $\sim$14 GPa. However, there are no corresponding changes in the 678 cm^{-1} peak. Because the 686 cm^{-1} peak is a low-intensity shoulder, subjected to less accurate fitting, we do not consider these nonlinearities as indicative of pressure-induced phase transitions.

TABLE I. Frequencies (ω), pressure dependencies ($\partial\omega_i/\partial P$), and Grüneisen parameters ($\gamma=-\partial \ln \omega_i/\partial \ln V$) of the observed Raman modes of LaB_6.

Mode	ω (cm^{-1}) at $P=0$	Pressure dependence (cm^{-1}/GPa)	γ
T_{2g}	678	3.57(8)	0.99(2)
	686	3.7(1)	1.01(3)
E_g	1111	8.5(3)	1.32(5)
	1129	8.0(6)	1.21(9)
	1150	6.6(8)	1.0(1)
A_{1g}	1253	Low pressure: 11.4(4); high pressure: 2.0(4)	1.53(7), 0.34(7)

The A_{1g} peak shifts initially at 11.4($\pm$0.5) cm^{-1}/GPa, then merges into the diamond Raman peak at pressures above 4 GPa and reappears above $\sim$15 GPa where the shift is 2.0($\pm$0.4) cm^{-1}/GPa. Our results are consistent with earlier measurements (Fig. 2), indicating a smooth but nonlinear variation in frequency with pressure between 0 and 20 GPa.

At low pressures the E_g mode is best fit with a triplet, although it appeared as a doublet in the single-crystal work.[14] With increasing pressure the intensity of this triplet is reduced and the ability to detect it diminished, such that it became impossible to fit any peaks above 8.6 GPa. There is

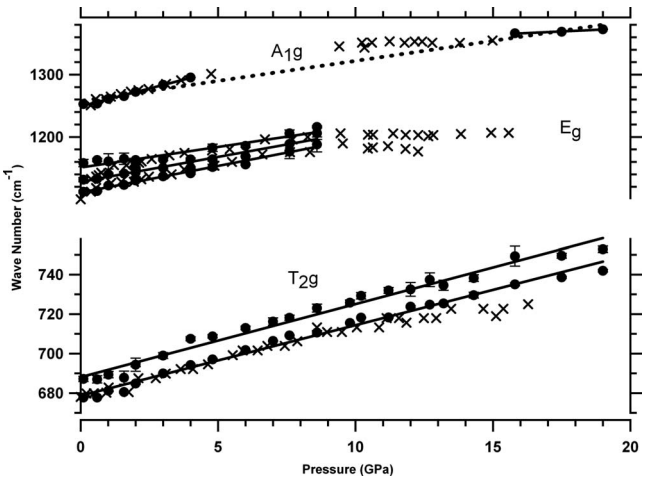

FIG. 2. Variation of A_{1g}, E_g, and T_{2g} mode frequencies with pressure: present measurements (filled circles with error bars: lines are linear fits) are compared with previous data (crosses) (Ref. 14).

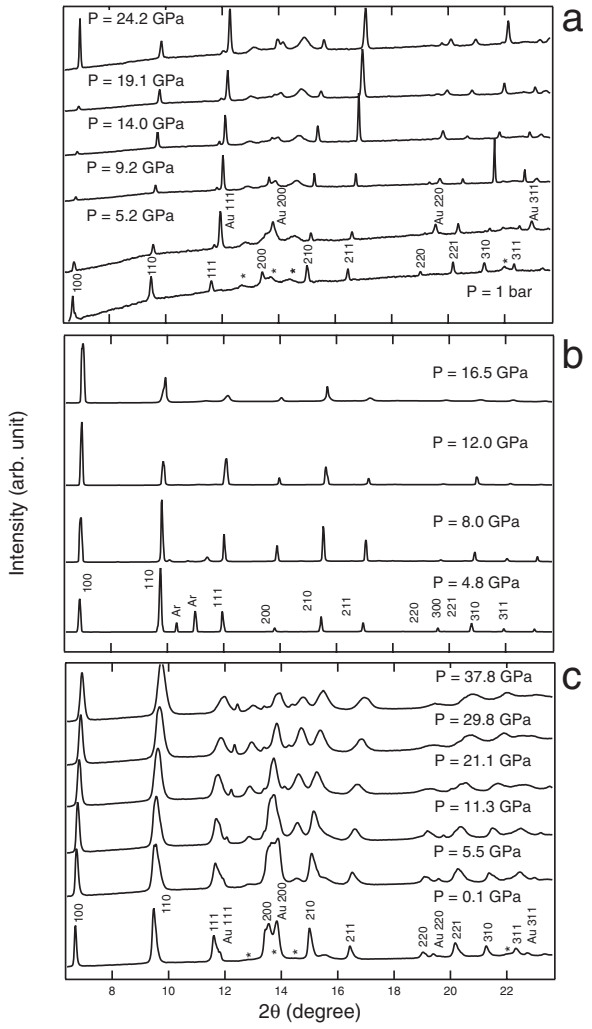

FIG. 3. X-ray diffraction patterns of LaB_6 compressed quasihydrostatically (a) in MEW to 24 GPa, (b) in argon to 16.5 GPa, and (c) nonhydrostatically to 37.8 GPa, with lines indexed based on the zero-pressure CsCl structure. Diffraction lines due to argon (Ar), stainless steel gasket (*) and gold are also identified.

again good agreement with the earlier study over the common range of pressures.

The powder x-ray diffraction patterns indicate that LaB_6 remains in the zero-pressure cubic crystal structure to pressures of at least 24.2 GPa (Fig. 3). Nonhydrostatic conditions can facilitate structural phase transitions that are otherwise kinetically hindered, but comparison of the patterns between quasihydrostatic and nonhydrostatic runs shows only broadening of diffraction lines—and no evidence of lines—in experiments with no pressure-transmitting medium to 37.8 GPa.

Except for the 200 line in the nonhydrostatic experiments, the diffraction patterns consist of nonoverlapping lines and we used single-peak fitting to determine d spacings and unit-cell volumes from 10 different lattice planes as a function of pressure. The resulting pressure-volume data, collected under compression and decompression with MEW and argon pressure media, show significant differences between hydrostatic and nonhydrostatic measurements (Fig. 4)—a well-known

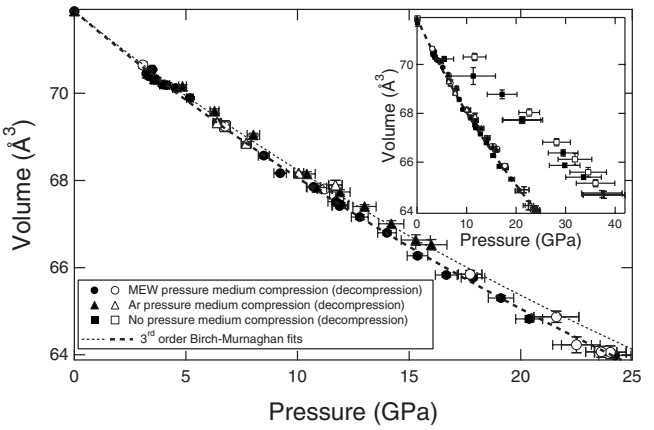

FIG. 4. Volume compression of LaB_6 at ambient temperature (*dotted line*: fit of data collected in Ar pressure medium; *dashed line*: fit of data in MEW pressure medium). *Inset*: quasihydrostatic data are compared with the results of compression without pressure medium.

effect (e.g., Refs. 24–27). The data sets collected with ethanol-methanol and argon are in reasonable agreement, within experimental uncertainties. However, the argon P-V curve appears to be slightly stiffer, consistent with others' estimates of the relative strengths of these two pressure media.[28,29] Large error bars under strongly nonhydrostatic conditions are due to line broadening from uniaxial strain. Another indication of uniaxial strain is the deviation of the nonhydrostatic data to large apparent volumes: this is due to the x-ray diffraction geometry, with data collected along the loading axis of the diamond anvils (i.e., diffracting-plane normals are nearly perpendicular to the loading axis and reflect minimum strains).

We analyzed the quasihydrostatic compression data separately (Table II) and, if we focus on the results of the more hydrostatic MEW measurements, the zero-pressure isothermal bulk modulus derived from fits to the third order Eulerian finite-strain (Birch-Murnaghan) equation of state compares well with the zero-pressure adiabatic bulk modulus $K_{0S}=163.2(\pm 1.5)$ GPa measured by ultrasonics.[4] This agreement implies that there is no pressure-induced phase transition with a volume change that can be resolved by the present measurements because, were there to be an isostructural phase transition, the pressure-volume measurements would yield a softer equation of state due to inclusion of data for the high-pressure (therefore smaller volume) phase: we find no evidence for such a bias. Moreover, a plot of normalized pressure $F=P/[3f(1+2f)^{5/2}]$ versus $f=0.5[(V_0/V)^{2/3}-1]$ (where V_0 is the unit-cell volume at am-

TABLE II. Parameters derived from 3rd order Birch-Murnaghan fit.

Data set	K_{T0} (GPa)	$(\partial K_T/\partial P)_{T0}$	Max P (GPa)	Pressure medium
1	164 ± 2	4.0 ± 0.4	24.2	MEW
2	173 ± 7	4.2 ± 1.5	16	Ar

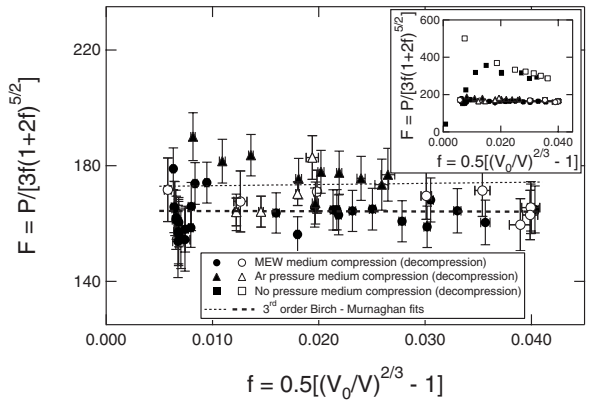

FIG. 5. Normalized pressure F as a function of Eulerian strain f for LaB_6: the intercept gives the zero-pressure bulk modulus K_{0T}, and the slope gives the deviation of the pressure derivative from $K'_{0T}=4$. *Dotted line*: fit of data set with Ar pressure medium; *dashed line*: fit of data set with MEW medium. *Inset*: data under quasihydrostatic conditions are compared with nonhydrostatic data.

bient conditions), which effectively gives the derivative of the equation of state, reveals no anomaly for either the methanol-ethanol-water or argon pressure medium (Fig. 5).

Previous *ab initio* electronic structure calculations show a minimum in the *d* band energy along the Γ-Σ-*M* direction of the Brillouin zone, at 0.8 mRy below the Fermi energy at ambient conditions ($V/V_0=1.0$).[14] This band rises with pressure and crosses the Fermi energy at a compression $V/V_0=0.92$, at which point an electronic topological transition (ETT) would be expected.[30] An ETT can be isostructural, and this compression is roughly that at which the previous single-crystal measurements indicated a break in slope in the pressure dependence of the Raman frequencies (better resolved than in the present study due to the measurements at 9–15 GPa).[14] Our Raman data on polycrystalline LaB_6, which compare well with the previous measurements on single crystals over the common pressure range, indicate a nonlinearity in the frequency shift of the A_{1g} mode (Fig. 2). The dotted line in Fig. 2 shows that a smooth trend, albeit with curvature, satisfies all of the observed data. Within the scatter of the data, the E_g mode shift documented in the previous single-crystal study is consistent with a smooth (but perhaps curved) trend.[14]

Taken together, we conclude that none of the existing data provide compelling evidence for any phase transition to at least 20–24 GPa at room temperature. From the present results, not only does the T_{2g} mode frequency increase smoothly with pressure to 20 GPa (Fig. 2), but the x-ray diffraction patterns exhibit a smooth pressure–volume relationship—with no diffraction lines—to comparable pressures (Figs. 3 and 4). Although our measurements may not be able to rule out less than 1%–3% of the sample transforming, or the sample undergoing an isostructural transition with less than 0.3%–0.5% volume change, they do not confirm the occurrence of an electronic or structural transition in LaB_6 at pressures below 24–38 GPa.

Raman measurements on polycrystalline LaB_6 are consistent with previous single-crystal measurements in documenting a smooth pressure dependence of the E_g, T_{2g}, and A_{1g} vibration-mode frequencies to pressures of about 20 GPa. High-resolution, synchrotron-based x-ray diffraction measurements using ethanol-methanol-water and argon pressure-transmitting media, as well as nonhydrostatic measurements with no medium, show no evidence of a phase transition from cubic to orthorhombic crystal structures as had previously been proposed based on data collected with a laboratory x-ray source.[14] The bulk modulus determined under quasihydrostatic conditions is in good agreement with independent elastic-constant measurements. We therefore find no signature of the subtle electronic phase transition near 10 GPa predicted by *ab initio* theory,[14] and the apparent disagreement between theory and experiments suggests that further studies are warranted in order to improve the ability to predict the onset of electronic topological transitions.

We thank Martin Kunz and Sander Caldwell as well as the ALS staff for support on beamline 12.2.2. The Advanced Light Source is supported by the U.S. Department of Energy under Contract No. DE-AC02-05CH11231. This research was partially supported by NSF Contract No. DMR-0605493 to COMPRES under NSF Cooperative Agreement No. EAR 06-49658, and by other grants from the NSF and DOE.

[1] T. Komatsubara *et al.*, J. Magn. Magn. Mater. **31-34**, 368 (1983).
[2] T. Kasuya *et al.*, J. Magn. Magn. Mater. **31-34**, 447 (1983).
[3] T. Kasuya *et al.*, J. Phys. (Paris), Colloq. **40**, C5–308 (1979).
[4] T. Tanaka *et al.*, Solid State Commun. **22**, 203 (1977).
[5] Z. Yahia *et al.*, J. Mol. Struct. **224**, 303 (1990).
[6] H. C. Longuet-Higgins and M. de V. Roberts, Proc. R. Soc. London, Ser. A **224**, 336 (1954).
[7] P. G. Perkins *et al.*, J. Phys. C **8**, 3558 (1975).
[8] A. J. Arko *et al.*, Int. J. Quantum Chem., Symp. **9**, 569 (1975).
[9] A. Hasegawa and A. Yananse, J. Phys. F: Met. Phys. **7**, 1245 (1977).
[10] V. A. Sidrov *et al.*, Sov. Phys. Solid State **32**, 1586 (1989).
[11] H. G. Smith *et al.*, Solid State Commun. **53**, 15 (1985).
[12] K. Takegahara and T. Kasuya, Solid State Commun. **53**, 21 (1985).
[13] H. A. Mook and R. M. Nicklow, Phys. Rev. B **20**, 1656 (1979).
[14] P. Teredesai *et al.*, Solid State Commun. **129**, 791 (2004).
[15] M. Nakasuji and H. Wada, J. Vac. Sci. Technol. **17**, 1367 (1980).
[16] M. Kunz *et al.*, J. Synchrotron Radiat. **12**, 650 (2005).
[17] H. K. Mao *et al.*, J. Geophys. Res. **91**, 4673 (1986).
[18] D. L. Heinz and R. Jeanloz, J. Appl. Phys. **55**, 885 (1984).
[19] S. H. Shim *et al.*, Earth Planet. Sci. Lett. **203**, 729 (2002).
[20] A. P. Hammersley *et al.*, High Press. Res. **14**, 235 (1996).
[21] R. L. Mills *et al.*, Rev. Sci. Instrum. **51**, 891 (1980).
[22] H. Scholz *et al.*, Solid State Commun. **18**, 1539 (1976).
[23] M. Ishii *et al.*, J. Phys. Soc. Jpn. **41**, 1075 (1976).
[24] T. S. Duffy *et al.*, Phys. Rev. B **60**, 15063 (1999).
[25] K. Takemura, J. Appl. Phys. **89**, 662 (2001).
[26] A. K. Singh, J. Phys. Chem. Solids **65**, 1589 (2004).
[27] D. J. Weidner *et al.*, Geophys. Res. Lett. **21**, 753 (1994).
[28] R. J. Angel *et al.*, J. Appl. Crystallogr. **40**, 26 (2007).
[29] S. Klotz *et al.*, J. Phys. D **42**, 075413 (2009).
[30] I. M. Lifshitz, Sov. Phys. JETP **11**, 1130 (1960).